JOURNAL OF AIRCRAFT
Vol. 41, No. 3, May–June 2004

Effects of Auxiliary Lift and Propulsion on Helicopter Vibration Reduction and Trim

Martin K. Sekula*
NASA Langley Research Center, Hampton, Virginia 23681
and
Farhan Gandhi†
The Pennsylvania State University, University Park, Pennsylvania 16802

This paper examines the vibration reductions caused by the introduction of auxiliary lift and propulsion, individually, as well as in combination, on a light [5800-lb (2640 kg)] helicopter with a four-bladed hingeless rotor, at flight speeds close to the maximum cruise velocity of the baseline helicopter. The changes in trim (vehicle orientations and control settings) because of auxiliary lift and propulsion are also examined in detail, and the fundamental mechanisms that produce the changes in trim and associated vibration reductions are identified. Based on results using a comprehensive aeroelastic analysis, it was concluded that auxiliary lift, alone, produces relatively small reductions in vibration. On the other hand, significant vibration reductions were obtained through auxiliary propulsion alone. A combination of lift and propulsion was most effective and reduced the vibration index by over 90%. It was also observed that auxiliary lift significantly reduces the main rotor thrust but increases the nose-down pitch attitude and tip-path-plane forward tilt to provide the required propulsive force. This increases the downwash through the rotor disk and requires a larger rotor longitudinal cyclic pitch input. In contrast, auxiliary propulsion that minimizes vibration produces little reduction in main rotor thrust, but results in a slightly nose-up pitch attitude (the auxiliary propulsion exceeds vehicle drag) along with a backward tilt of the tip-path plane. This decreases the downwash through the rotor disk and requires a smaller rotor longitudinal cyclic pitch input. A combination of auxiliary lift and propulsion minimizes vibration results in an even larger backward tilt of the tip-path plane and a net upwash through the rotor disk. The rotor collective pitch undergoes little change as a result of auxiliary lift, even though the main rotor thrust is decreased. In contrast, for auxiliary propulsion it decreases significantly even though the rotor thrust undergoes only small reductions. This counterintuitive observation is explained. The reduced downwash with auxiliary propulsion, or upwash with combined lift and propulsion, puts the rotor in a partial autorotation state, drastically reducing the induced drag, main rotor torque, and power. Auxiliary lift produces modest reductions in main rotor power, primarily because of a reduced profile drag associated with lower rotor loading. Because the rotor loading is lower with auxiliary lift than with auxiliary propulsion, but larger vibration reductions are produced with the latter, it can be deduced that vibration reductions are less a result of "unloading" of the rotor per se and more because of overall changes in trim, especially the reduction in longitudinal cyclic pitch (seen with auxiliary propulsion).

Nomenclature

a	=	lift-curve slope
C_{M_x}	=	nondimensional rotor rolling moment
C_{M_y}	=	nondimensional rotor pitching moment
C_T	=	nondimensional rotor thrust
D_F	=	fuselage drag
F_x, F_y, F_z	=	main rotor axial, side, and vertical hub forces
F_x^A	=	auxiliary propulsion
F_z^A	=	auxiliary lift
f	=	equivalent flat-plate area of the fuselage
J_v	=	composite vibration index
M_x, M_y, M_z	=	main rotor roll, pitch, and yaw hub moments
m_0	=	blade mass/length
N	=	main rotor blades number
R	=	main rotor radius
S_{ht}	=	horizontal tail planform area
T	=	total thrust or lift
T_R	=	total rotor thrust
T_R^{Full}	=	total rotor thrust with auxiliary lift and propulsion
T_R^{Lift}	=	total rotor thrust with the inclusion of auxiliary lift
$T_R^{\text{Prop.}}$	=	total rotor thrust with the inclusion of auxiliary propulsion
V	=	helicopter forward velocity
W	=	helicopter weight
w_{tip}	=	equivalent elastic blade-tip flap response
w_0, w_{1c}, w_{1s}	=	equivalent elastic blade coning, 1/rev longitudinal and lateral tip flapping response
x, y, z	=	axial, side, and vertical offsets
α_s	=	forward shaft tilt
$\beta_0, \beta_{1c}, \beta_{1s}$	=	coning and 1/rev longitudinal and lateral rigid flap response
θ_{tr}	=	tail rotor collective pitch
θ_{1c}	=	main rotor lateral cyclic pitch
θ_{1s}	=	main rotor longitudinal cyclic pitch
θ_{75}	=	main rotor collective pitch
λ	=	inflow ratio
μ	=	advance ratio, $V/\Omega R$
ν_β	=	first rotating blade flap frequency
ρ	=	air density
σ	=	rotor solidity
ϕ_s	=	side shaft tilt
Ω	=	main rotor speed of rotation

Received 14 January 2003; revision received 10 July 2003; accepted for publication 10 July 2003.

*Research Engineer, U.S. Army Vehicle Technology Directorate.
†Associate Professor, Rotorcraft Center of Excellence, Department of Aerospace Engineering, 229 Hammond Building.

Subscripts

cg	=	pertaining to the helicopter center of gravity
ht	=	pertaining to the horizontal tail
tr	=	pertaining to the tail rotor

Superscripts

0	=	zeroth-harmonic or steady rotor hub loads
$4P$	=	4/rev vibratory rotor hub loads
-	=	nondimensionalized

Introduction

IN high-speed cruise conditions helicopters can experience severe vibration levels caused by the rotor blades operating in a non-axisymmetric aerodynamic environment. The periodic inertial and aerodynamic loading experienced by the rotor blades is transmitted, in part, to the rotor hub at harmonics of the blade passage frequency $N\Omega$. The vibratory loads transmitted to the rotor hub can result in significant crew and passenger discomfort, increased component fatigue and maintenance requirements, and reduced effectiveness of sensitive equipment and weapon systems for military helicopters. Eventually, at some cruise speed the onset of compressibility effects on the advancing blade and stall on the retreating blade increases blade loads, pitch link loads, hub vibrations, and power requirements to unacceptable levels and limits the flight envelope.

In general, three different approaches have been pursued over the past several decades to improve performance of rotary-wing aircraft in high-speed cruise conditions: 1) passive methods, 2) active control concepts, and 3) changes in vehicle configuration. Passive methods include the use of vibration absorbers and isolation devices and structural and aerodynamic optimization of rotor blades. Although these methods have had some success in reducing hub vibratory loads, they generally involve a weight penalty, and their performance can degrade with change in operating conditions. Active rotor control including higher harmonic blade pitch control through the swashplate and individual blade control (IBC) implemented through blade-root pitch actuators in the rotating frame or trailing-edge flaps, for example, can be extremely effective in reducing vibration and can have the ability to adapt to changes in operating condition. However, the actuation and power requirements and the pitch link loads can be quite large, and the complexity involved can be considerable (for example, in the transfer of power to the rotating system through a slip ring, in the case of IBC). Another active strategy, active control of structural response (ACSR), places actuators in the airframe, or between the pylon and the fuselage, to cancel the incoming N/rev hub loads. ACSR can reduce airframe vibration levels, but also requires high power and actuation force and leaves the dynamic stresses experienced by the rotor blades unaltered. In general, the emphasis of the passive and active approaches just summarized was to reduce vibration levels within the existing flight envelope, not to expand the flight envelope to any significant degree.

In contrast, changes in vehicle configuration, such as tilting the rotors forward into "propeller mode" (as in the case of tilt-rotor aircraft) or introducing auxiliary lift and propulsive devices (as in the case of compound helicopters), were primarily intended to increase the maximum operating speed. In a tilt-rotor aircraft the rotor is tilted into propeller mode in moderate- to high-speed flight, and a fixed-wing provides all of the necessary lift. This produces a mostly axisymmetric flow through the rotor disk, thereby eliminating the source of vibration, as well as the problems of compressibility and stall that set maximum speed limits on a conventional helicopter. In compound helicopters auxiliary propulsive devices (tractor or pusher propellers, jet engines, etc.) and lift devices (fixed-wings) partially offload the rotor in high-speed flight and thereby delay the onset of stall and compressibility effects to even higher flight speeds. Tilt rotors and compound helicopters, by modifying the aerodynamic environment experienced by conventional helicopter rotors at high speeds, alleviate the source that limits the flight speed and produces vibration. This is in contrast to the active and passive approaches discussed in the preceding paragraph, which mitigate the adverse effects (the vibration levels) of high-speed flight, but not the cause (the adverse aerodynamic environment that produces them). A tilt-rotor aircraft can achieve higher maximum speeds and experiences lower vibration levels than a compound helicopter. However, there is a significantly larger price to be paid in complexity and cost. Helicopter compounding, through the introduction of auxiliary lift (lift compounding), auxiliary propulsion (thrust compounding), or both in combination (full compounding), is considered to be a more evolutionary advancement[1] and has an advantage in that existing conventional helicopters can be retrofitted relatively quickly, easily, and at lower cost.[1,2] However, even with compound helicopters, factors such as weight of the wings, weight and complexity of auxiliary propulsion devices (and associated transmissions), reduced payload, and reduced efficiency of the rotor at low flight speeds caused by wing interference must be considered. In fact, compound aircraft are reported to have an increased productivity only for a limited class of high-speed, long-range missions.[1,2] Consequently, despite extensive research, especially in the 1950s–1970s, no compound aircraft in the west progressed beyond the prototype phase to production. A summary of some of the major research programs on compound helicopters is provided in Ref. 3.

Notwithstanding the fact that compound helicopters have never reached production and acquisition in the West, their technological success—in terms of their ability to increase the maximum flight speed, reduce vibration, eliminate stall, improve maneuverability, reduce power, and improve productivity for certain missions—was clearly established. With regards to reduction in vibration, there have been numerous studies in the literature that have reported decreased vibration levels as a result of the inclusion of auxiliary lift and auxiliary propulsion (for example, see Refs. 4–10). Auxiliary lift and propulsion reduces aircraft vibration levels over a wide range of flight speeds. Thus, substantially lower levels are observed compared to conventional (uncompounded) counterparts flying in the prestall range. In addition, the vibration levels for the compound configurations were also acceptable at higher speeds, far beyond those achievable by conventional helicopters. In the literature, however, effects of compounding on vibration levels are available only for a limited number of configurations—the Lockheed XH-51,[5] the Sikorsky S-61,[7] and the Westland Lynx,[9,10] for example. Furthermore, even for a given aircraft, reductions in vibration level are typically provided for a specified auxiliary lift or propulsion, and detailed analyses of vibration levels as a function of auxiliary lift and auxiliary propulsion, either individually or in combination, are not readily available. And although there is a general intuitive understanding of the underlying physical mechanisms that bring about vibration reductions, a rigorous comparison of the mechanisms involved when using auxiliary lift and auxiliary propulsion, and the associated changes in vehicle trim in each case, has not been presented. This is, in part, because of the unavailability of modern computational tools and comprehensive rotorcraft analyses in the 1950s–1970s, when most of the research programs on compound helicopters were underway.

In the present study a comprehensive rotorcraft analysis is used to 1) evaluate the reductions in rotor hub vibrations achievable with increasing levels of auxiliary lift and auxiliary propulsion, both individually as well as in combination; 2) examine and understand the overall effects of increasing levels of auxiliary lift and auxiliary propulsion, in modifying vehicle trim (orientation and controls); and 3) conduct an in-depth diagnosis and develop a fundamental understanding of the complex underlying mechanisms at work that produced the changes in trim and reductions in vibration for the optimum (maximum vibration reduction) auxiliary lift, auxiliary propulsion, and the combination of the two. The study is based on a light-weight BO-105 type helicopter with a four-bladed hingeless rotor, at an advance ratio of 0.35. This advance ratio corresponds to a cruise speed of approximately 135 kn, which is close to the maximum speed of the BO-105. Thus, the emphasis is on analyzing the changes in trim and reductions in vibration possible with the introduction of increasing levels of auxiliary forces, near the edge of the flight envelope of a conventional helicopter—not demonstrating that the flight speed can be increased (this has already been established in

the literature). Further, a fundamental understanding of the physical mechanisms is sought, without focusing too much on design details such as effects of location of wing or auxiliary propulsive device, their weight, additional drag, associated pitching moments, etc.

Analysis

To evaluate the effect of auxiliary lift and propulsion in modifying the helicopter trim and reducing the rotor hub vibratory loads, a comprehensive rotorcraft aeroelastic analysis based on the University of Maryland Advanced Rotorcraft Code (UMARC) formulation[11] is used. In the analysis the rotor blades are assumed to be long, slender beams with uniform cross-section properties, undergoing elastic flap and lag bending and elastic torsion deformation. The blades are discretized along the span using the finite element method, employing six elements, each with four flap degrees of freedom, four lag degrees of freedom, and three torsion degrees of freedom. Blade-element theory is used to calculate the sectional aerodynamic loads acting on the rotor blades (assumed to have a NACA 0012 airfoil), with a table look-up routine (that accounts for compressibility effects and static stall) used to obtain the circulatory lift, drag, and pitching moment. The model also accounts for the noncirculatory lift and pitching moment and the reverse flow region on the retreating side of the disk. The discretized blade equations of motion are transformed to modal space (two flap modes, two lag modes, and two torsion modes are used) to reduce computational cost, and the blade periodic response in forward flight is calculated using the temporal finite element method. After calculating the periodic response, the blade loads can then be integrated along the span to obtain the blade root forces and moments, and these can be integrated around the azimuth and summed over the N blades of the rotor to calculate the steady rotor hub loads (the hub forces F_x^0, F_y^0, and F_z^0 and moments M_x^0, M_y^0, and M_z^0). The rotor hub loads appear in the vehicle equilibrium (trim) equations and impact the vehicle orientation (pitch attitude or longitudinal shaft tilt α_s and roll attitude or lateral shaft tilt ϕ_s) and control settings (main rotor collective pitch θ_{75}, longitudinal cyclic pitch θ_{1s}, lateral cyclic pitch θ_{1c}, and tail rotor collective pitch θ_{tr}). Because any change in orientation and controls will affect the blade response and rotor hub loads, evaluation of blade response and vehicle orientation and controls is carried out iteratively in a coupled response-trim calculation procedure. The iterative process continues until convergence, with the converged solution yielding the vehicle orientation and controls, blade periodic response, as well as the steady and the vibratory rotor hub loads. Figure 1 shows all of the forces and moments acting on the vehicle, and the vehicle equilibrium equations [Eq. (1)] are then obtained by summing the forces and moments at the rotor hub.

In the present study the influence of auxiliary lift and propulsion on the vehicle trim and rotor hub vibratory loads was examined for a light (5800 lb gross weight) BO-105 type helicopter with a four-bladed hingeless rotor. The rotor and fuselage properties used in the simulations are presented in Tables 1 and 2. The vehicle equilibrium equations are given next and have been properly modified to include the auxiliary forces:

$$\sum F_x = 0 = F_x^0 \cos\alpha_s - F_z^0 \sin\alpha_s + D_F + \underline{F_x^A} \tag{1a}$$

$$\sum F_y = 0 = F_y^0 \cos\phi_s + F_z^0 \sin\phi_s + T_{\text{tr}} \tag{1b}$$

$$\sum F_z = 0 = F_z^0 \cos\phi_s \cos\alpha_s + F_x^0 \sin\alpha_s - F_y^0 \sin\phi_s - W - T_{\text{ht}} + \underline{F_z^A} \tag{1c}$$

Table 1 Rotor properties

Property	Value
Radius, R	16.2 ft
Chord, c	1.296 ft
Angular velocity, Ω	40.123 rad/s
Solidity, σ	0.1
Number of blade, N	4
Lock number, γ	6.34
Airfoil	NACA 0012
Hub offset	4%
Blade mass, m_0	0.135 slugs/ft
Blade cross-section stiffness	
Flap, EI_{yy}	1.25×10^5 lb-ft^2
Lag, EI_{zz}	3.47×10^5 lb-ft^2
Torsion, GJ	5.72×10^4 lb-ft^2
Nondimensional rotating frequencies	
1st flap	1.15
2nd flap	3.40
1st lag	0.75
2nd lag	4.37
1st torsion	4.59
2nd torsion	13.6
Reference lift coefficient, a	5.73
Aerodynamic hub cutout	10%

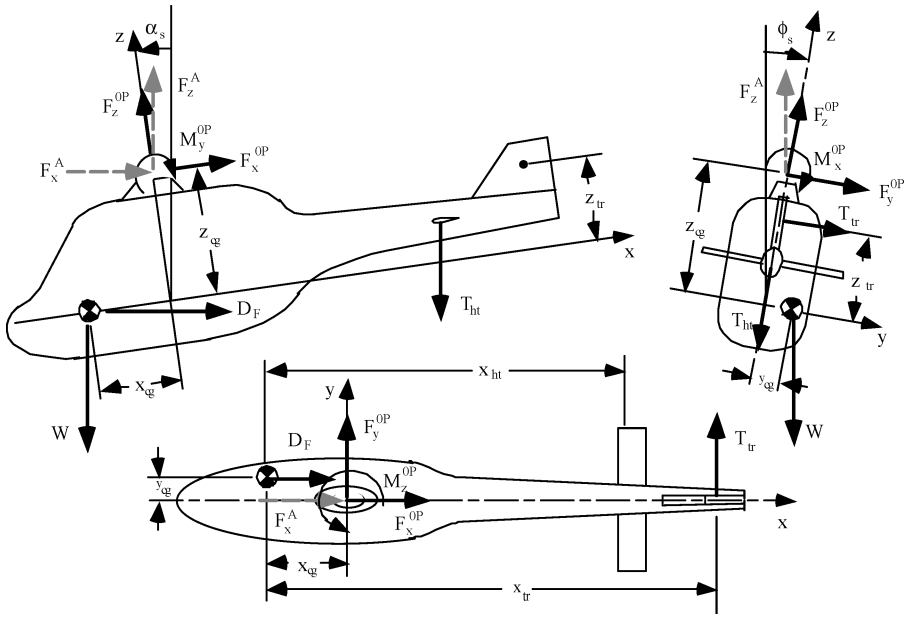

Fig. 1 Equilibrium forces and moments acting on the helicopter.

Table 2 Helicopter properties

Property	Value
Weight, W	5800 lb
Fuselage flat-plate area, f	8.24 ft^2
Center of gravity location with respect to the rotor hub	
x_{cg}	0 ft
y_{cg}	0 ft
z_{cg}	3.24 ft
Horizontal tail properties	
Area, S_{ht}	9.07 ft^2
x_{ht}	15.39 ft
Lift coefficient, a_{ht}	6.0
Tail-rotor properties	
Radius, R_{tr}	3.24 ft
Angular velocity ratio, Ω_{tr}/Ω	5
Solidity, σ_{tr}	0.15
x_{tr}	19.44 ft
z_{tr}	3.24 ft
Lift coefficient, a_{tr}	6.0

$$\sum M_x = 0 = M_x^0 + W z_{cg} \sin\phi_s \tag{1d}$$

$$\sum M_y = 0 = M_y^0 - D_F z_{cg} \cos\alpha_s + W z_{cg} \sin\alpha_s + T_{ht} x_{ht} \tag{1e}$$

$$\sum M_z = 0 = M_z^0 + T_{tr} x_{tr} \tag{1f}$$

In Eq. (1) T_{ht} is the download on the horizontal tail ($T_{ht} = \frac{1}{2}\rho V^2 S_{ht} a_{ht} \alpha_s$). Although the fuselage drag can in general vary with changes in vehicle pitch attitude, it is assumed to be independent of vehicle attitude in the present analysis ($D_F = \frac{1}{2}\rho V^2 f$, where the equivalent flat-plate area f is assumed to be independent of α_s). Fuselage lift, side force, and moments are assumed to be zero. The underlined terms represent the auxiliary propulsion F_x^A and auxiliary lift F_z^A. The location of the vehicle c.g. relative to the rotor hub is (x_{cg}, y_{cg}, z_{cg}), as shown in Fig. 1. However, in the present analysis it is assumed that the c.g. is directly below the hub ($x_{cg} = 0$, $y_{cg} = 0$, and only $z_{cg} \neq 0$), and this has resulted in the moment equilibrium relations being somewhat simplified. The tail-rotor vertical offset below the main rotor hub $z_{cg} - z_{tr}$ is zero, so that the tail rotor does not produce any rolling moment about the rotor hub. The longitudinal offset of the tail rotor relative to the helicopter c.g. is x_{tr}.

Clearly, auxiliary propulsion F_x^A and auxiliary lift F_z^A will have an effect on the vehicle trim (vehicle orientation and controls), which in turn will have an influence on the blade response and the rotor hub vibrations. In essence, the auxiliary lift and propulsion provide redundant controls that allow the change of the vehicle trim (determined from equilibrium considerations and probably suboptimal from a hub vibration standpoint for a conventional helicopter) to a state that is more favorable for hub vibratory load considerations. In the present study the maximum auxiliary lift considered is 4000 lb or approximately 70% of the total helicopter weight (a reasonable choice for compound lift helicopters; for example, see Refs. 6 and 12). The maximum auxiliary propulsion considered is 850 lb, which is 65% higher than the fuselage drag at advance ratio 0.35 (where the analysis is carried out) and thus represents an autogyro configuration (with an effective rearward tilt of the main rotor thrust).

In an actual aircraft introduction of auxiliary lift F_z^A through a fixed wing or auxiliary thrust F_x^A through devices such as propellers or jet engines would also result in a pitching moment about the rotor hub (as a result of longitudinal offset of the wing aerodynamic center fore/aft of the rotor hub and vertical offset of the auxiliary propulsion device above/below the rotor hub). However, because the magnitude of the associated pitching moment would be totally configuration specific it is neglected in the present study. Neglecting the pitching moments is tantamount to assuming that the auxiliary lift and propulsion device have zero longitudinal and vertical offsets, respectively, relative to the rotor hub. Further, small changes in orientation of the auxiliary propulsion force with change in aircraft pitch attitude are neglected, and the auxiliary lift is assumed to be independent of vehicle pitch attitude as well (which could be achieved by equipping the wings with variable pitch or controllable flaps). Also, weight, drag, or interference effects associated with the wings or auxiliary propulsion devices are neglected, as these would also be device and configuration specific. Although introducing auxiliary propulsion and lift forces F_x^A and F_z^A without precisely specifying how they would be applied is a simplification, it allows the effects of the auxiliary forces to be isolated and provides a very fundamental understanding of the mechanism causing the changes in trim and reduction in vibration. This is the focus of the present study, and the conclusions drawn are meant to be broad and general rather than limited to a specific design (with given auxiliary lift and/or propulsion device weight, size, placement, drag, interference effects, additional pitching moment, etc.), as has usually been the case in the literature.

To examine the effectiveness of using auxiliary lift and propulsion in the fixed system in reducing helicopter hub vibratory loads, a composite vibration index J_v, which considers all six components of vibratory hub loads, is defined as follows:

$$J_v = 100 \sqrt{\sum_{i=1}^{6} \left(\bar{F}_i^{4P}\right)^2 \Big/ \sum_{i=1}^{6} \left(\bar{F}_i^{4P}\right)^2_{\text{baseline}}} \tag{2}$$

In Eq. (2), the overbar indicates that the three forces and the three moments are nondimensionalized (forces by $m_0\Omega^2 R^2$ and the moments using $m_0\Omega^2 R^3$). It is seen that $J_v = 100$ for the baseline helicopter, and a vibration index of less than 100 indicates an overall decrease in vibration while values greater than 100 indicate an increase.

Results and Discussion

The effectiveness of auxiliary lift (lift compounding), auxiliary propulsion (thrust compounding), or both in combination (full compounding) in reducing vibratory hub loads is examined for a BO-105 type light helicopter (5800 lb gross weight), with a four-bladed hingeless rotor. The baseline helicopter rotor-fuselage properties are provided in Tables 1 and 2. The analysis is carried out at an advance ratio of $\mu = 0.35$. (This corresponds to a flight speed of approximately 135 kn, which is close to the maximum speed of the helicopter.) At this flight speed it is seen from Fig. 2 that angles of attack around the rotor disk for the baseline helicopter do not exceed 12 deg (on the retreating side), so that the NACA 0012 airfoil (static stall of around 13 deg) is not in a stalled condition. Although a dynamic-stall aerodynamic model would be necessary for higher advance ratios or vehicle weight, the quasi-steady table look-up approach (which includes compressibility effects) used in the present study is adequate for the flight condition examined. In the following sections observations that were made during the course of this study are presented. In the first section the vibration reductions

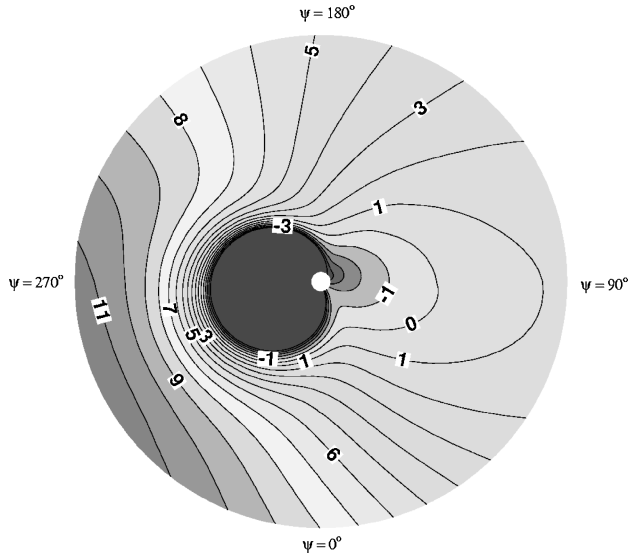

Fig. 2 Blade-sectional angles of attack around the rotor disk for baseline helicopter.

achievable with increasing levels of auxiliary lift and propulsion are presented, and the optimal levels of auxiliary lift and propulsion that would provide maximum vibration reductions, when used individually as well as in combination, are identified. The next section discusses the changes in vehicle attitude and control settings (trim) caused by the introduction of auxiliary lift and propulsion. In the last three sections the three optimal cases (optimal auxiliary lift, optimal auxiliary propulsion, and optimal combination of auxiliary lift and propulsion) are analyzed in further detail to understand the underlying mechanisms in play.

Vibration Reduction with Auxiliary Lift and Propulsion

Reduction in vibration index, as a function of increasing values of auxiliary lift F_z^A and auxiliary propulsion F_x^A, is shown in Fig. 3. From this figure three cases of interest are selected for detailed analysis: 1) optimum auxiliary lift, 2) optimum auxiliary propulsion, and 3) optimum combination of auxiliary lift and propulsion (these are marked on the figure). The vibration indices for each of these cases along with the corresponding auxiliary lift and propulsion values are provided in Table 3. From this table and Fig. 3 it can be seen that auxiliary propulsion is substantially more effective at reducing vibration than auxiliary lift. A similar observation was reported in Ref. 13, but reductions in vibration using different levels of auxiliary lift or propulsion were never actually compared. Figure 3 also indicates that at high auxiliary propulsion levels the effectiveness of auxiliary lift in reducing vibration increases significantly and that maximum vibration reductions are achieved when auxiliary propulsion and lift are used in combination (a fully compounded configuration).

Table 4 presents the individual vibratory hub load components for the three optimum cases identified. It is seen that the optimal auxiliary lift ($F_z^A = 2400$ lb) produced an approximately 35% reduction in vibratory torque, modest 12% reductions in vibratory pitching and rolling moments, and 20% reductions in the vibratory in-plane forces, while the vibratory vertical force increased by 10%. The optimal auxiliary propulsion ($F_x^A = -800$ lb) produced 73% reductions in the vibratory in-plane hub forces and a 35% reduction in the vibratory torque. It also yielded modest reductions of just over 10% in the vibratory pitching and rolling moments, while producing a 20% increase in the vibratory vertical force. Optimal full compounding ($F_z^A = 4000$ lb, $F_x^A = -720$ lb) reduced all components of vibratory hub loads by 80–95%.

Table 3 Vibration index for a conventional helicopter and configurations with auxiliary lift and propulsion

Vibration index	Baseline	Auxiliary lift	Auxiliary propulsion	Combined lift and propulsion
F_x^A, lb	0	0	−800	−720
F_z^A, lb	0	2400	0	4000
J_v	100	83.6	43.6	7.65

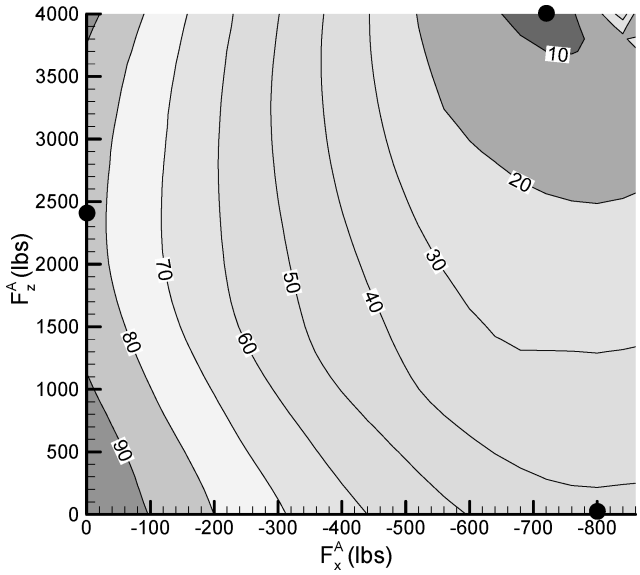

Fig. 3 Vibration index J_v vs auxiliary lift and propulsion.

Table 4 Vibratory hub loads for a conventional helicopter and auxiliary lift and propulsion configurations

Vibratory hub loads	Baseline	Auxiliary lift		Auxiliary propulsion		Combined lift and propulsion	
F_x^A, lb	0	0		−800		−720	
F_z^A, lb	0	2400		0		4000	
		Load	%	Load	%	Load	%
F_x^{4P}, lb	133	105	79.3	35.8	26.9	8.23	6.19
F_y^{4P}, lb	146	122	83.3	39.2	26.8	5.99	4.10
F_z^{4P}, lb	52.1	57.4	110	62.0	118.8	11.0	21.0
M_x^{4P}, ft-lb	485	426	87.8	435	89.7	62.0	12.8
M_y^{4P}, ft-lb	520	455	87.5	462	88.8	69.0	13.3
M_z^{4P}, ft-lb	391	257	65.7	248	63.4	26.7	6.83

Table 5 Control settings for a conventional helicopter and auxiliary lift and propulsion configurations

Control and power	Baseline	Auxiliary lift	Auxiliary propulsion	Combined lift and propulsion
F_x^A, lb	0	0	−800	−720
F_z^A, lb	0	2400	0	4000
θ_{75}, deg	8.92	8.28	4.37	−0.85
θ_{1c}, deg	3.30	2.73	1.69	0
θ_{1s}, deg	−7.27	−6.66	−3.29	1.19
θ_{tr}, deg	4.38	3.83	0.75	0.57
α_s, deg	3.88	6.15	−1.30	−2.64
ϕ_s, deg	−1.20	−2.38	0.71	−0.62
λ	0.0340	0.0442	0.0018	−0.0133
P_{rotor}, hp	491	429	83.5	64.2
P_{total}, hp	491	429	414	362

The vibration results presented in Fig. 3 were obtained using a linear (Drees) inflow model.[14] Although the actual vibratory loads (for any combination of auxiliary lift and propulsion) would be higher if a free wake were considered in computing the rotor inflow, a limited number of results with the inclusion of the free-wake are provided in the Appendix to demonstrate that the trends presented in Fig. 3 are valid. Figure 3 was generated by calculating vibratory loads in 100-lb increments in auxiliary lift and 40-lb increments in auxiliary propulsion. Thus, over 900 different combinations of auxiliary lift and propulsion were considered. Because computing the free-wake geometry for such a large number of cases would be prohibitively expensive, vibratory loads, with the inclusion of a free wake (in Fig. A1), are shown only for variation in auxiliary propulsion level. It is seen that the reductions in vibratory loads for increasing auxiliary propulsion are generally very similar using both the Drees inflow model as well as the free-wake analysis from Ref. 15, although the actual levels differ considerably. The only significant differences seen are for auxiliary propulsion levels are in the range of 300–475 lb, in which case the inclusion of the free wake gives lesser vibration reductions. However, it can be seen from Fig. A2 that for these values of auxiliary propulsion the longitudinal shaft tilt angle is very small (between 1.5 and 0 deg) so that the tip vortices of the rotor wake are in very close proximity to the rotor disk.

The attitude and control settings for the baseline helicopter in steady level flight are shown in Table 5. These are compared to corresponding values (same flight condition) for the three optimum compound configurations just identified. Table 5 shows that while optimum lift compounding produces some modest changes in the trim solution, thrust and full compounding drastically alter the trim solution. The physics of why these trim changes occur are discussed in the following sections.

Changes in Trim with Increasing Auxiliary Lift and Propulsion

In this section some general observations are made about the effect of increasing levels of auxiliary lift and propulsion on helicopter

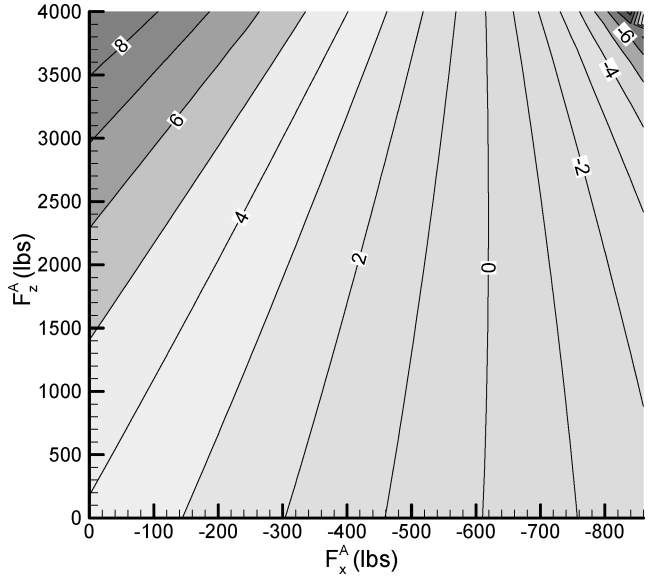

Fig. 4 Longitudinal shaft tilt α_s (nose-down pitch attitude) vs auxiliary lift and propulsion.

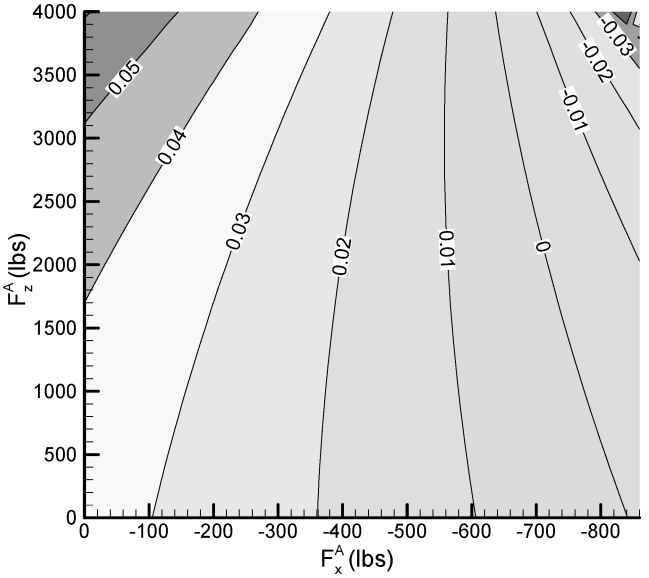

Fig. 6 Inflow ratio λ vs auxiliary lift and propulsion.

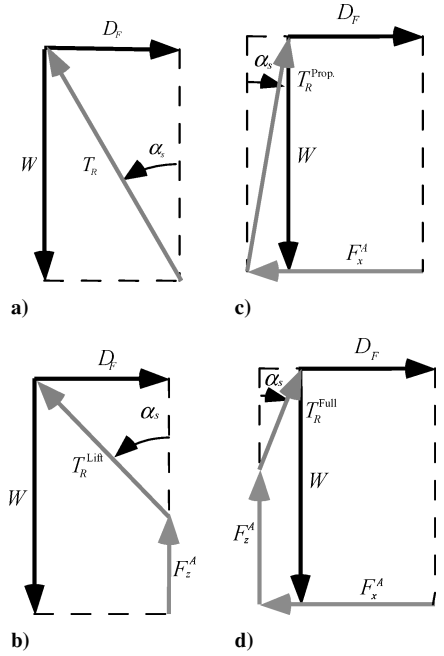

Fig. 5 Physics governing the influence of auxiliary lift and propulsion on α_s.

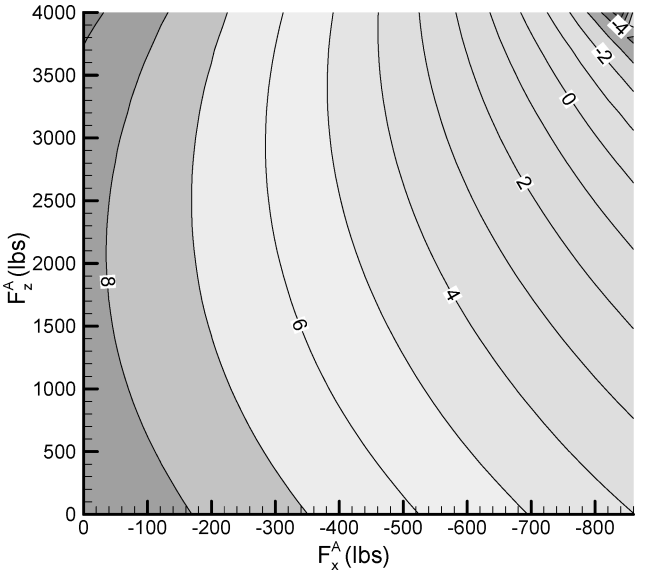

Fig. 7 Collective pitch θ_{75} vs auxiliary lift and propulsion.

attitude and control settings. Figure 4 shows the variation of longitudinal shaft tilt α_s for increasing auxiliary lift and propulsion. Clearly, auxiliary lift causes an increase in forward shaft tilt, whereas auxiliary propulsion causes it to decrease. This can be explained by considering Fig. 5. In Fig. 5a the rotor thrust T_R for the baseline case has to balance the vehicle weight W and provide the propulsive force to overcome the drag D_F. For a compound lift configuration part of the weight is balanced by the auxiliary lift F_z^A (Fig. 5b). However, all of the propulsive force still has to be provided by the main rotor, and this requires a net forward tilt of the rotor thrust vector T_R^{Lift}. An increase in the forward shaft tilt contributes to this. For a compound thrust configuration, in contrast, because an auxiliary propulsion device (and not the main rotor) provides the required propulsive thrust, little longitudinal tilting of the rotor thrust vector $T_R^{\text{Prop.}}$ is required (as seen in Fig. 5c). In fact, if the auxiliary propulsion F_x^A is greater than the aircraft drag the main rotor thrust and consequently the shaft may actually tilt rearward, as seen in Fig. 5c.

The addition of auxiliary lift to auxiliary propulsion should further increase this effect and produce an even larger rearward tilt of the resulting main rotor thrust vector T_R^{Full} (see Fig. 5d).

The changes in α_s have a direct impact on the value of the inflow through the rotor disk (see Fig. 6). For auxiliary lift the inflow (downwash) through the disk increases as the shaft tilts more forward for larger values of F_z^A. Conversely, for auxiliary propulsion the inflow decreases as the shaft assumes a more vertical position and even becomes negative when the shaft tilts back for larger values of F_x^A. Figure 7 shows the variation of main rotor collective pitch for increasing values of auxiliary lift and propulsion. It is clear that auxiliary lift produces larger reductions in the magnitude of the main rotor thrust vector than auxiliary propulsion (compare Figs. 5b and 5c to Fig. 5a). From this viewpoint lift compounding would intuitively be expected to produce larger reductions in the collective pitch θ_{75}. Figure 7, however, shows the reverse to be true, with increasing auxiliary lift producing little reduction in θ_{75} and increasing auxiliary propulsion producing significant reductions. Figure 8 shows variation of main rotor longitudinal cyclic pitch θ_{1s}. It also reduces in magnitude (become less negative) for increasing values of auxiliary propulsion F_x^A and shows lesser sensitivity to changes in auxiliary lift F_z^A. These characteristics (variations in inflow, collective pitch,

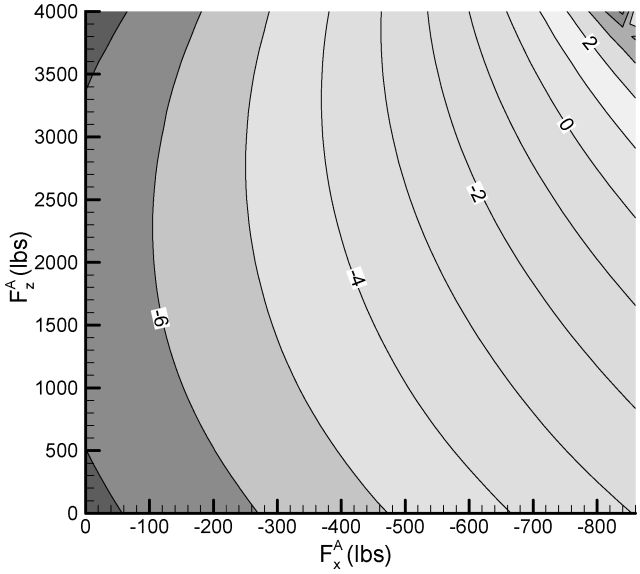

Fig. 8 Longitudinal cyclic pitch θ_{1s} vs auxiliary lift and propulsion.

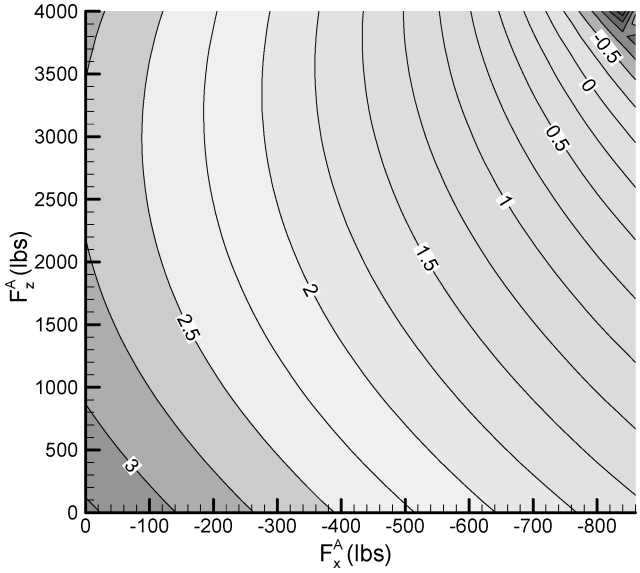

Fig. 9 Lateral cyclic pitch θ_{1c} vs auxiliary lift and propulsion.

and longitudinal cyclic pitch) are explained in greater detail in the following sections.

The lateral cyclic pitch θ_{1c} shows moderate reductions for increasing values of auxiliary lift and propulsion (see Fig. 9). The tail rotor collective pitch θ_{tr} reduces appreciably as the auxiliary propulsion increases, but shows little sensitivity to increasing auxiliary lift (see Fig. 10). Figure 11 indicates that for increasing auxiliary propulsion the lateral shaft tilt ϕ_s significantly reduces and eventually changes sign. The effect of auxiliary lift on ϕ_s is strongly dependent on the auxiliary propulsion level. For low auxiliary propulsion levels ϕ_s increases for increasing auxiliary lift, but for high auxiliary propulsion levels ϕ_s shows little sensitivity to increasing auxiliary lift.

Detailed Analysis of Optimal Auxiliary Lift Case

In this section the optimal auxiliary lift case of $F_z^A = 2400$ lb is analyzed in greater detail. From Table 5 it is seen that the main rotor pitch controls θ_{75}, θ_{1s}, and θ_{1c} do not show major changes relative to the baseline configuration. The most significant trim change occurs in the increased forward shaft tilt α_s. These observations can be explained by first examining changes in the steady rotor forces and moments and then considering their effects on vehicle equilibrium. From Table 6 it is seen that lift compounding drastically reduces the steady rotor thrust F_z^0 necessary to maintain level flight while

Table 6 Steady rotor hub loads for a conventional helicopter and auxiliary lift and propulsion configurations

Steady hub loads	Baseline	Auxiliary lift	Auxiliary propulsion	Combined lift and propulsion
F_x^A, lb	0	0	−800	−720
F_z^A, lb	0	2400	0	4000
F_x^0, lb	−105	−108	155	129
F_y^0, lb	−220	−144	−130	−27. 6
F_z^0, lb	6060	3811	5730	1653
M_x^0, ft-lb	396	778	−229	203
M_y^0, ft-lb	−3151	−5969	3279	4949
M_z^0, ft-lb	−6729	−5881	−1144	−880

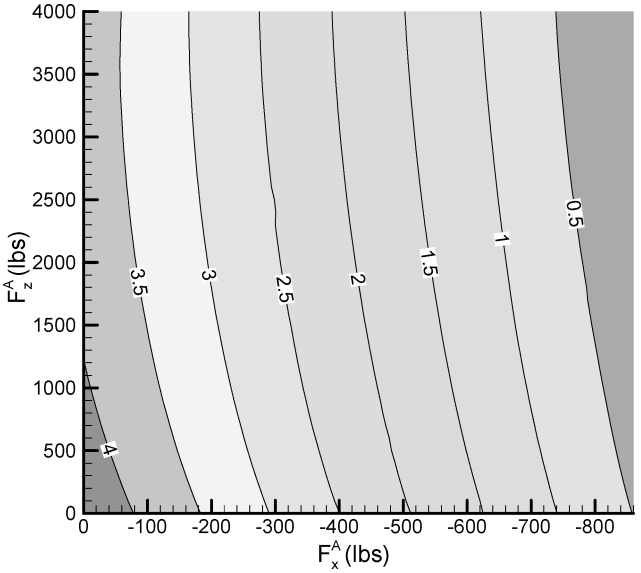

Fig. 10 Tail-rotor collective pitch θ_{tr} vs auxiliary lift and propulsion.

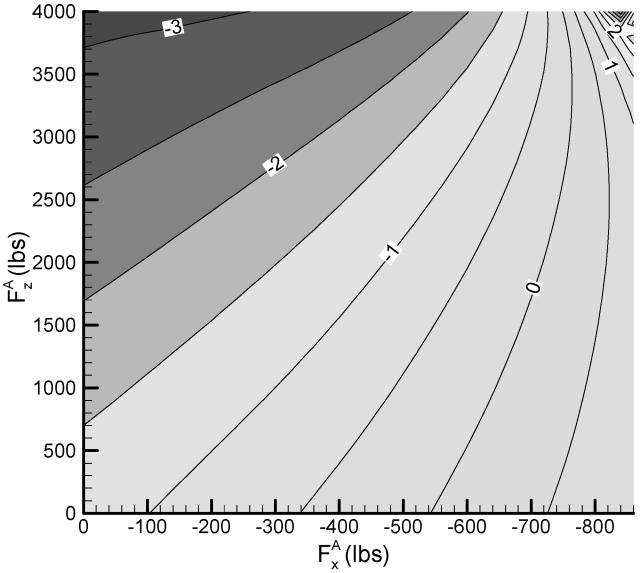

Fig. 11 Lateral shaft tilt ϕ_s vs auxiliary lift and propulsion.

maintaining approximately the same level of the rotor drag F_x^0 (relative to the baseline). All of the rotor forces and moments are in the rotor hub reference frame. Considering equilibrium of vertical forces (Table 7), it is seen that the auxiliary lift augments the reduced rotor thrust (or causes F_z^0 to reduce) to balance the vehicle weight and a slightly increased horizontal tail downward force (caused by increased α_s). Considering equilibrium of forces in the x direction (Table 8), it is seen that none of the individual components changed

Table 7 Decomposition of the vertical force equilibrium (force in pounds)

Vertical force components	Baseline	Auxiliary lift	Auxiliary propulsion	Combined lift and propulsion
F_x^A, lb	0	0	−800	−720
F_z^A, lb	0	2400	0	4000
$F_z^0 \cos(\alpha_s)\cos(\phi_s)$	6044	3786	5728	1651
$+F_x^0 \sin(\alpha_s)$	−7.14	−11.6	−3.51	−5.93
$-W$	−5800	−5800	−5800	−5800
$-T_{\text{ht}}$	−230	−365	77.0	157
$-F_y^0 \sin(\phi_s)$	−4.59	−5.99	1.62	−0.30
$+F_z^A$	0.00	2400	0.00	4000

Table 8 Decomposition of the longitudinal equilibrium (force in pounds)

Longitudinal force components	Baseline	Auxiliary lift	Auxiliary propulsion	Combined lift and propulsion
F_x^A, lb	0	0	−800	−720
F_z^A, lb	0	2400	0	4000
$F_x^0 \cos(\alpha_s)$	−105	−108	155	129
$+D_f$	515	515	515	515
$-F_z^0 \sin(\alpha_s)$	−410	−408	130	76.2
$+F_x^A$	0	0	−800	−720

significantly, relative to the baseline helicopter. For the propulsive component of the rotor thrust, $F_z^0 \sin\alpha_s$, to be relatively unchanged despite a large reduction in the rotor thrust F_z^0 itself, an increase in the forward shaft tilt α_s must occur. The change in α_s increases the inflow ratio (Table 5), which in turn is responsible for a smaller than expected reduction in the collective pitch. The rotor thrust, of course, is a radial and azimuthal integration of blade-sectional lift, which depends on blade-sectional angles of attack, not just the blade pitch setting. Increased inflow caused by increased forward shaft tilt increases the inflow angle at any blade section and reduces the net angle of attack, and consequently the rotor thrust, even if the pitch setting itself is not significantly changed (see Fig. 12). Examining the basic analytical expression for collective pitch of an untwisted blade undergoing rigid-body flapping rotations, obtained from blade element theory, is also very illuminative in explaining the small change in collective pitch:

$$\theta_0 = \left[3\Big/\left(1+\tfrac{3}{2}\mu^2\right)\right]\left[2C_T/\sigma a - (\mu/2)\theta_{1s} + \lambda/2\right] \qquad (3)$$

Equation (3) shows that although the collective pitch would be expected to reduce with decreasing rotor thrust (or thrust coefficient C_T) an increase in the inflow ratio λ would negate this effect. The increased downward force on the horizontal tail caused by the nose-down aircraft attitude (increased α_s) slightly reduces the effectiveness of lift compounding because the auxiliary lift needs to counteract the increased tail download. However, this could be alleviated by adjusting the incidence angle of the horizontal tail. In the present case (unchanged horizontal tail incidence) the increased α_s results in the horizontal tail producing a larger nose-up moment. The larger α_s also produces an additional increase in the nose-up pitching moment of the vehicle c.g. about the rotor hub (see Table 9) by causing a relative rearward shift in the c.g. location. To satisfy pitching-moment equilibrium, the main rotor now produces a larger nose-down pitching moment M_y^0, as compared to the baseline (see Tables 6 and 9).

Considering the analytical expressions next and relating the rotor pitching- and rolling-moment coefficients to longitudinal and lateral cyclic flapping (or longitudinal and lateral tilting of the tip path plane),

$$C_{M_y} = -(\sigma a/2\gamma)\left(\nu_\beta^2 - 1\right)\beta_{1c} \qquad (4)$$

$$C_{M_x} = (\sigma a/2\gamma)\left(\nu_\beta^2 - 1\right)\beta_{1s} \qquad (5)$$

Table 9 Decomposition of the pitching-moment equilibrium (moments in feet/pound)

Pitching moment components	Baseline	Auxiliary lift	Auxiliary propulsion	Combined lift and propulsion
F_x^A, lb	0	0	−800	−720
F_z^A, lb	0	2400	0	4000
M_y^0	−3151	−5969	3279	4949
$-D_F z_{\text{cg}} \cos(\alpha_s)$	−1666	−1660	−1670	−1668
$+W z_{\text{gc}} \sin(\alpha_s)$	1272	2013	−425	−866
$+T_{\text{ht}} x_{\text{ht}}$	3546	5620	−1184	−2414

Table 10 Blade-tip flap response (degree)

Flap response	Baseline	Auxiliary lift	Auxiliary propulsion	Combined lift and propulsion
F_x^A, lb	0	0	−800	−720
F_z^A, lb	0	2400	0	4000
$\bar{w}_0$	3.49	2.53	2.89	0.62
$\bar{w}_{1c}$	1.05	1.98	−0.96	−1.61
$\bar{w}_{1s}$	0.214	0.457	−0.339	−0.181

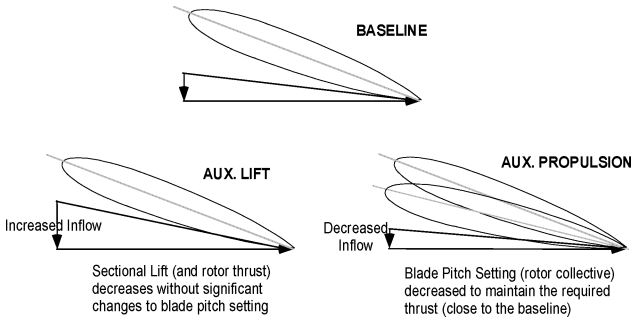

Fig. 12 Effect of inflow on blade-sectional angle of attack and lift.

it can be expected that the larger nose-down rotor pitching moment (more negative M_y^0 or more negative C_{M_y}) for the compound lift configuration would produce a larger forward tilt of the tip path plane [larger β_{1c}; see Eq. (4)]. Because Eqs. (4) and (5) are derived for a rigid flapping rotor, they do not directly apply to the present analysis wherein the blades are assumed to undergo elastic flap and lag bending and elastic torsion deformations. However, it is expected that the fundamental physics would be unchanged. Thus, in the present analysis the blade-tip flapping response $\bar{w}_{\text{tip}}$ (w_{tip} nondimensionalized by the rotor radius R) is expressed in terms of its Fourier series components, with the collective component $\bar{w}_0$ equivalent to the rotor coning β_0 and the cyclic components $\bar{w}_{1c}$ and $\bar{w}_{1s}$ equivalent to the longitudinal and lateral tilts of the tip path plane β_{1c} and β_{1s}, respectively.

The collective and 1/rev tip flapping response, calculated as just described, is presented in Table 10. The compound lift configuration is seen to produce a larger forward tilt of the tip path plane $\bar{w}_{1c}$ than the baseline. This is consistent with the substantially larger nose-down rotor pitching moment (compare baseline and compound lift values in Table 6).

While lift compounding produces an increase in longitudinal cyclic flap $\bar{w}_{1c}$, relative to the baseline, it produces a decrease in the magnitude of the longitudinal cyclic pitch θ_{1s} (see Table 5), which is generally thought to drive the longitudinal flap response. Examining the longitudinal cyclic flap expression next (based on blade element theory for rigid-body out-of-plane flap rotations),

$$\beta_{1c} = \left[1\Big/\left(1-\tfrac{1}{2}\mu^2\right)\right]\left[2\mu\left(\lambda - \tfrac{4}{3}\theta_0\right) - \left(1+\tfrac{3}{2}\mu^2\right)\theta_{1s}\right] \qquad (6)$$

it is seen that whereas an increase in the magnitude of longitudinal cyclic pitch (more negative θ_{1s}) can increase the longitudinal cyclic flap, it is the larger inflow ratio λ for the auxiliary lift case that actually produces an increase in longitudinal cyclic flapping.

Table 11 Decomposition of the rolling-moment equilibrium (moments in feet/pound)

Rolling moment components	Baseline	Auxiliary lift	Auxiliary propulsion	Combined lift and propulsion
F_x^A, lb	0	0	−800	−720
F_z^A, lb	0	2400	0	4000
M_x^0	396	778	−230	203
$+W z_{cg} \sin(\phi_s)$	−393	−782	234	−202

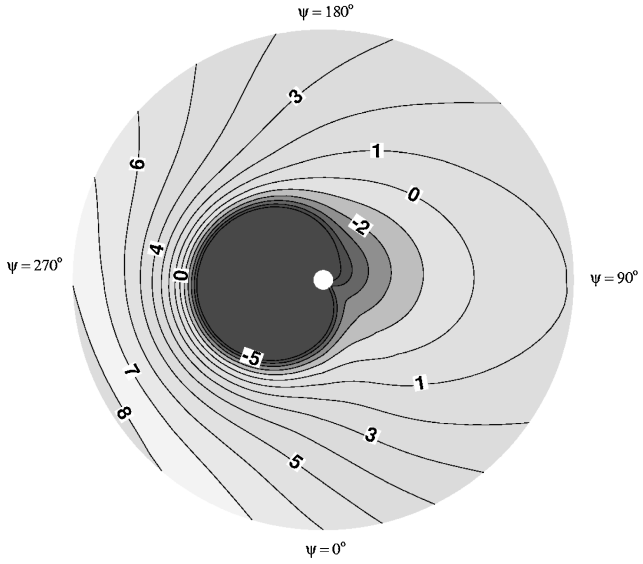

Fig. 13 Blade-sectional angle of attack around the rotor disk for optimum auxiliary lift.

Equation (5) indicates that a larger rotor rolling moment would produce an increase in lateral cyclic flapping. Table 6 shows that auxiliary lift results in an increase in the rotor roll-left moment M_x^0 relative to the baseline, and a corresponding increase in lateral cyclic flapping $\bar{w}_{1s}$ is observed in Table 10. With auxiliary lift the increased roll-left rotor moment increases the leftward shaft tilt (ϕ_s has become more negative relative to the baseline as seen in Table 5). This moves the vehicle c.g. relative to the rotor hub (in the wind axes system), which in turn creates an opposing roll-right moment to satisfy roll equilibrium (see Table 11). The increased leftward tilt of the main rotor thrust vector (through increases in magnitude of ϕ_s and $\bar{w}_{1s}$) is required because the magnitude of the main rotor thrust has decreased, and the larger leftward tilt now counteracts the tail rotor thrust.

Figure 13 shows the blade-sectional angle of attack around the rotor disk when the optimal auxiliary lift is used. Compared to Fig. 2, it is observed that the angles of attack have reduced significantly relative to the baseline. This is to be expected because the main rotor is producing a substantially lower thrust, and presumably the lower angles of attack are responsible for the moderate reduction seen in main rotor torque (Table 6). A main rotor torque reduction would in turn produce a reduction in the tail-rotor thrust (which counteracts the main rotor torque). Accordingly, the tail-rotor collective pitch is seen to have reduced, relative to the baseline (see Table 5).

Detailed Analysis of Optimal Auxiliary Propulsion Case

In this section the optimal auxiliary propulsion case of $F_x^A = -800$ lb is analyzed in greater detail. From Table 5 it is seen that there are significant changes in all of the orientation and control parameters, relative to the baseline. As in the case of auxiliary lift, these changes can be explained by examining the changes in steady rotor forces and moments and their influence on vehicle equilibrium. Because the auxiliary propulsion of 800 lb is greater than the fuselage drag (515 lb), the rotor shaft tilts rearward (nose-up attitude), as seen in Table 5. From Table 8 it is seen how the rearward shaft tilt and the resultant change in direction of the main rotor propulsive thrust ($F_z^0 \sin\alpha_s$ and $F_x^0 \cos\alpha_s$ terms), relative to the baseline, satisfies equilibrium of forces in the x direction in the presence of the auxiliary propulsion. The slight rearward longitudinal shaft tilt reduced the inflow ratio to almost zero (see Table 5). The reduced inflow drastically reduces the induced drag on the blade sections so that the rotor is approaching autorotation state, and this drastically reduces the steady rotor torque M_z^0 (Table 6). Correspondingly, a significant reduction in tail-rotor collective is observed (Table 5). The magnitude of the main rotor thrust F_z^0 itself has not undergone the significant reduction seen with auxiliary lift (Table 6), although it shows a slight reduction because the nose-up pitch attitude resulted in the horizontal tail producing an upload instead of a download, and in addition the main rotor does not have to provide the propulsive thrust. It is somewhat counterintuitive that despite no significant change in the magnitude of the main rotor thrust the main rotor collective θ_{75} undergoes a drastic reduction relative to the baseline (see Table 5). This can be attributed to the significant reduction in inflow that results in a generic blade section requiring a lower pitch setting to produce a comparable lift (see Fig. 12), and this in turn results in the rotor producing a thrust comparable to the baseline, but at a much lower collective pitch [see also Eq. (3)]. The change in α_s also had a significant effect on vehicle pitching-moment equilibrium. Compared with the baseline (see Table 9), the pitching moments as a result of the c.g. location relative to the hub (in the wind axes system) and the horizontal tail are reversed in sign. This is counteracted by a change in the sign of the main rotor pitching moment M_y^0 from nose down to nose up (see Tables 6 and 9). Consistent with Eq. (4), the reversal in sign of the main rotor pitching moment also results in a reversal in sign of the longitudinal cyclic flapping, so that there is now a backward tilt of the tip path plane relative to the shaft. [$\bar{w}_{1c}$ has become negative; (Table 10)]. For a conventional helicopter a negative longitudinal cyclic pitch (negative θ_{1s}) prevents the rotor from flapping or blowing back in the wind and then forces it to tilt forward. Because the tip path lane no longer has to be tilted forward for the compound thrust case, the longitudinal cyclic pitch input is reduced substantially compared to the baseline (see Table 5).

Table 6 shows that the main rotor roll moment M_x^0 also reverses sign relative to the baseline. A corresponding change in lateral cyclic flapping [based on Eq. (5)] is obtained (Table 10). The change in sign of the rotor roll moment produces a corresponding reversal of the lateral shaft tilt ϕ_s relative to the baseline (Table 5), and so the location of the vehicle center of gravity creates an opposing moment about the rotor hub to counter the negative rotor rolling moment and satisfy the rolling-moment equilibrium (see Table 11). The significant change in trim caused by auxiliary propulsion changes the blade-section angles of attack around the disk (compare Figs. 2 and 14), with significant reductions seen on the retreating side of the rotor disk. The reduction in main rotor torque M_z^0 with auxiliary propulsion (see Table 6) significantly reduced the main rotor power (from 491 to 84 hp with auxiliary propulsion; Table 5). This was mainly, because as the rotor disk straightens and then tilts slightly backward the upwash through the rotor caused by the freestream reduces the induced power of the rotor and puts it in near autorotative state. However, when the power caused by auxiliary propulsion is itself considered, the total power (414 Hp) reduces by a more modest amount.

Much larger reductions in vibration caused by auxiliary propulsion (than auxiliary lift) suggest that vibration reductions are not as much caused by a reduced loading of the main rotor (an idea that has been given much credence in the literature; for example, see Refs. 4, 6, 12, 16, and 17), as they are caused by reductions in cyclic rotor pitch control inputs (seen with the introduction of auxiliary propulsion). Though the swashplate cyclic pitch input is at the fundamental rotor frequency Ω, it does contribute to higher harmonic loading on the blade and to hub vibrations, so that a reduction in cyclic pitch can be expected to produce a corresponding reduction in vibrations. The present vibration reduction study, though, is conducted in the prestall regime (close

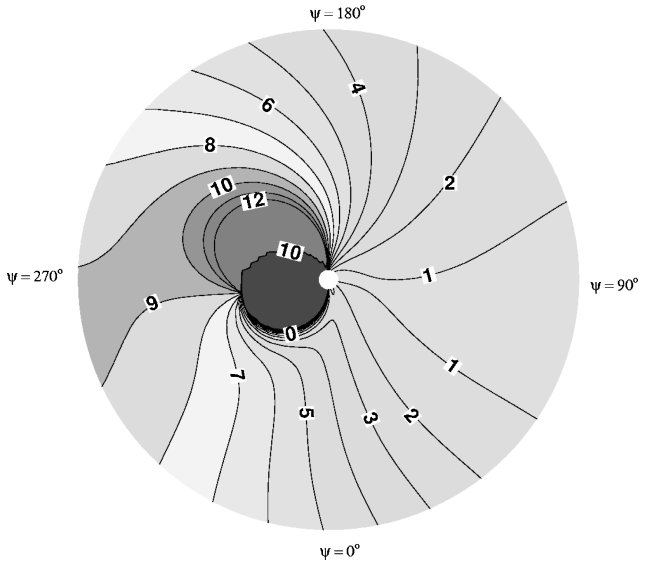

Fig. 14 Blade-sectional angle of attack around the rotor disk for optimum auxiliary thrust.

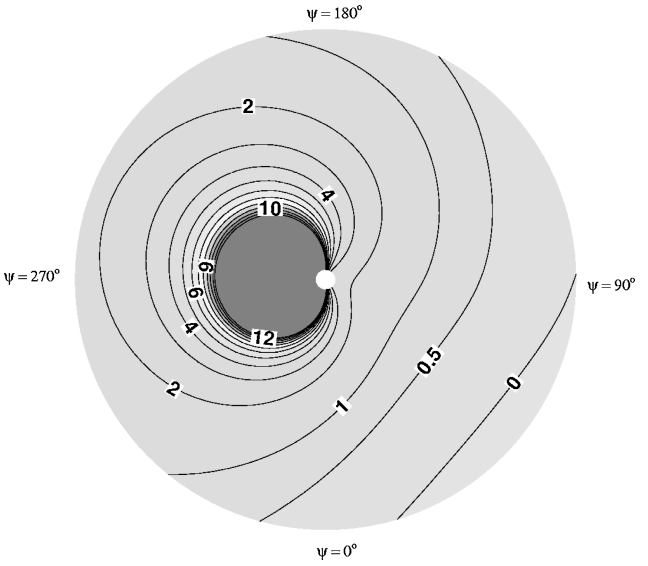

Fig. 15 Blade-sectional angle of attack around the rotor disk for the combination of auxiliary lift and thrust.

to the maximum speed of a conventional helicopter), and at flight speeds that would place a conventional helicopter in the poststall regime, unloading of the main rotor is likely to assume greater significance.

Note the key distinctions between the auxiliary lift and the auxiliary propulsion cases. Auxiliary lift, even while significantly reducing the main rotor thrust, caused the thrust vector to tilt forward and produced some increase in the forward tilt of the tip path plane $\bar{w}_{1c}$, the nose-down attitude of the aircraft α_s, and the longitudinal cyclic pitch θ_{1s}. But these parameters did not show the kind of gross changes from the baseline helicopter that were observed when auxiliary propulsion was used. With auxiliary propulsion the main rotor thrust and the tip path plane now actually assume a slight rearward tilt, and the aircraft itself assumes a slight nose-up pitch attitude. Because the main rotor thrust is allowed to blow back in the wind and does not have to be forced to tilt forward, the longitudinal cyclic pitch θ_{1s} is significantly reduced. Also, the near-vertical position of the rotor shaft reduces the downwash through the disk and results in a reduction of the main rotor collective pitch. Although there is significant offloading of the main rotor with auxiliary lift and little offloading with auxiliary propulsion, much larger reductions in collective pitch are seen in the latter case. Large reductions in cyclic pitch are also seen with auxiliary propulsion. Because vibration reductions are much greater with auxiliary propulsion than with auxiliary lift, it might be reasonable to deduce that reduction in cyclic pitch input, more than the unloading of the rotor per se, is producing the reductions in vibration. With auxiliary lift the unloading of the main rotor and the lower blade-sectional angles of attack around the rotor disk produce modest reductions in main rotor power (mostly profile power reductions). In contrast, with auxiliary propulsion the near-zero inflow puts the rotor in a partial autorotative state, and very large reductions in main rotor power are observed (induced power reductions).

Analysis of Optimal Full Compounding Case

In this section the optimal full compound case, using a combination of an auxiliary propulsive force $F_x^A = -720$ lb and an auxiliary lift force $F_z^A = 4000$ lb, is analyzed in greater detail. It was observed earlier that auxiliary lift only produces moderate changes in trim and reductions in vibration, whereas auxiliary propulsion produces more drastic changes in trim and larger reductions in vibration. In this section it will be seen that full compounding produces changes in trim that are qualitatively similar to the auxiliary propulsion only case. Nevertheless, there are distinctions, and it is these distinctions that are emphasized in the present section.

The presence of a very large auxiliary lift causes the main rotor steady vertical force F_z^0 to drastically reduce (Table 6). As in the preceding section, the auxiliary propulsion is greater than the fuselage drag causing a rearward rotor shaft tilt, or nose-up attitude (see Table 5), to produce equilibrium of forces in the x direction (Table 8). The rearward shaft tilt, however, is significantly greater than that when auxiliary propulsion alone was used (although F_x^A is now smaller) because the reduced magnitude of the main rotor thrust (caused by the auxiliary lift) must tilt back more to satisfy the longitudinal force equilibrium. The increased rearward shaft tilt now results in a net upwash through the rotor disk (see negative inflow in Table 5) and further reduces the main rotor steady torque (Table 6) and the main rotor power (Table 5), because of the further reductions in induced losses. Even when the power caused by auxiliary propulsion is added, the total power is the lowest of any of the configurations and over 25% lower than the baseline. Although this estimate neglects the transmission losses associated with the auxiliary propulsion, there would be other benefits such as additional reductions in fuselage drag caused by more level pitch attitude, relative to the baseline (Table 5). The low main rotor thrust (or loading), along with reduced cyclic pitch input, results in very low angles of attack around the disk, as seen in Fig. 15 (compare with Fig. 2, or even with Figs. 13 and 14). The low rotor thrust, along with a net upwash through the disk, also results in a very small collective pitch requirement. In fact, the collective pitch is observed to be negative for the configuration considered (see Table 5).

As with the auxiliary propulsion only case, the nose-up vehicle attitude (rearward shaft tilt) has the vehicle c.g. and the horizontal tail producing nose-down moments about the rotor hub. These moments are larger than the corresponding moments for the auxiliary propulsion only case (see Table 9) since the rearward shaft tilt has increased. To satisfy the pitching-moment equilibrium, the rotor now produces a larger nose-up pitching moment (Table 9). The larger rotor pitching moment would be expected to result in a larger longitudinal cyclic flapping [Eq. (4)], relative to the auxiliary propulsion only case, and this is observed in Table 10. Full compounding is also seen to result in the main rotor rolling moment being significantly reduced, relative to the baseline case (see Table 6), and this produces a reduction in the lateral shaft tilt ϕ_s (see Table 5), required to satisfy the vehicle rolling moment equilibrium (see Table 11).

Conclusions

The present study evaluates the reductions in helicopter vibratory hub loads that could be obtained through the introduction of

auxiliary lift and propulsion, individually as well as in combination. The study is conducted on a lightweight BO-105 type helicopter with a four-bladed hingeless rotor, at an advance ratio of 0.35 (approximately 135 kn), which is close to the maximum speed of the baseline (uncompounded) configuration. The study also thoroughly examines the changes in trim (control settings and vehicle orientation) caused by auxiliary lift and propulsion and provides a fundamental understanding of the physical mechanisms that bring about the changes in trim and the associated reductions in vibratory loads. Based on the numerical results and analysis in this study, the following major conclusions can be drawn:

1) Auxiliary lift alone produces relatively modest reductions in hub vibratory loads (vibration index only reduced to 84% of the baseline level with optimal lift). In comparison, auxiliary propulsion alone is much more effective in reducing the hub vibrations (vibration index reduced to 44% with optimal propulsion). An optimal combination of auxiliary lift and propulsion can produce the largest reductions in vibratory hub loads (composite vibration index reduced to 8%, with reductions of 80–95% in the individual vibratory hub load components).

2) Introduction of auxiliary lift results in a significant decrease in the magnitude and an increase in the forward tilting of the main rotor thrust vector, which no longer has to support the entire helicopter weight, but is still required to provide the entire propulsive force. Consequently, there are increases in both the forward shaft tilt (nose-down aircraft attitude) as well as the longitudinal cyclic flapping (forward tilt of tip path plane) relative to the baseline configuration. In contrast, auxiliary propulsion would result in a smaller change in the magnitude and a decrease in the forward tilting of the main rotor thrust vector, which still supports the entire helicopter weight, but is no longer required to provide the entire propulsive force. In fact, if the auxiliary propulsion exceeds the vehicle drag the main rotor thrust vector would have a net rearward tilt. Thus, auxiliary propulsion reduces the forward shaft tilt or even produces a slight rearward shaft tilt (nose-up aircraft attitude), and the tip path plane can be tilted back slightly as well (negative longitudinal cyclic flapping). With auxiliary lift the larger forward tilt of the tip path plane (increased longitudinal cyclic flapping) requires a larger longitudinal cyclic pitch input (θ_{1s} more negative). With auxiliary propulsion, in contrast, because the tip path plane does not have to tilt forward, the longitudinal cyclic pitch input (negative θ_{1s}) is significantly reduced.

3) The main rotor thrust was smallest when the optimal combination of auxiliary lift and propulsion (which produced the lowest hub vibrations) was used, followed by the optimal auxiliary lift and optimal auxiliary propulsion configurations, in that order. When both auxiliary lift and propulsion are used in combination, the weight is supported in significant part by the former, whereas the propulsive requirements are provided in entirety by the latter.

4) Differences in shaft tilt between the different configurations resulted in large changes in the inflow through the rotor disk. For the auxiliary lift case the increased forward shaft tilt increased the downwash. The reverse was true for the auxiliary propulsion case. For the optimal combination of auxiliary lift and propulsion case, the even larger rearward shaft tilt actually resulted in an upwash through the rotor disk.

5) Even though auxiliary lift substantially reduces the main rotor thrust and auxiliary propulsion produces much smaller reductions in the main rotor thrust relative to the baseline, the main rotor collective pitch is drastically reduced for the auxiliary propulsion case and shows only very modest reductions for the auxiliary lift case. This phenomenon is caused by the changes in rotor inflow for the two cases. The large inflow in the auxiliary lift case reduces the blade-sectional angles of attack and thus the rotor thrust, without substantially reducing the main rotor collective. In other words, even without large reductions in collective pitch significant reductions in main rotor thrust are obtained because of the increased inflow. In contrast, the rotor inflow in the auxiliary propulsion case is significantly reduced and requires a large reduction in the main rotor collective if the main rotor thrust is still to be more or less comparable to (and not far in excess of) the baseline. When auxiliary lift and propulsion are used in combination, the upwash through the rotor disk, along with a reduced magnitude of the main rotor thrust, requires even greater reductions in the collective pitch, which can now become negative.

6) The reduced inflow for the auxiliary propulsion and full compound cases puts the rotor in a partial autorotation condition and drastically reduces the blade-sectional induced drag and the main rotor torque and power. Even with the inclusion of power associated with auxiliary propulsion, the overall power requirement is considerably lower than the baseline. Main rotor power reductions with auxiliary lift are much more modest and appear to be caused by a reduction in the blade-sectional profile drag. (The rotor has lower loading than the baseline and auxiliary propulsion case, hence lower sectional angles of attack.)

7) Vibration reductions with auxiliary lift are much smaller than those with auxiliary propulsion, even though the rotor is offloaded substantially in the first case, and only marginally, in the second. This suggests that vibration reductions are less because of "unloading" of the main rotor (an idea commonly suggested in the literature) and might have more to do with the reductions in longitudinal cyclic pitch, associated with the introduction of auxiliary propulsion. More generally, the following statement could be made: Vehicle orientation and control inputs are determined from equilibrium considerations and might be suboptimal from a hub vibration standpoint. The introduction of auxiliary "redundant" lift and propulsion forces allows the choice of a trim state that is more beneficial from a vibration standpoint.

Appendix: Free Wake Model Comparison

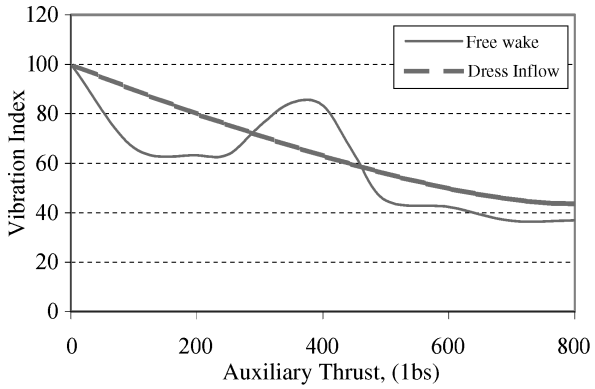

Fig. A1 Vibration index J_v vs auxiliary thrust.

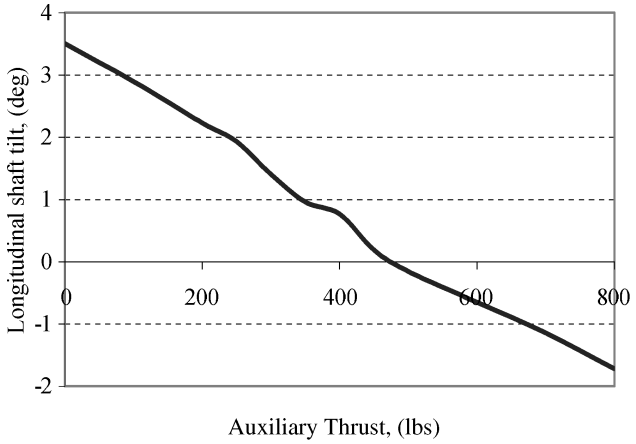

Fig. A2 Forward shaft tilt vs auxiliary thrust using a free-wake model.

Acknowledgment

The authors gratefully acknowledge Phuriwat Anusonti-Inthra of the Penn State University Rotorcraft Center of Excellence for his assistance with the free-wake simulations.

References

[1]Fradenburgh, E. A., "Rotorcraft Designs of the Year 2000," *AGARD, Rotorcraft Design for Operations*, Paper 17, 1987.

[2]Balmford, D. E. H., and Bender, B. S., "The Compound Helicopter—A Concept Revisited," *Proceedings of the 25th European Rotorcraft Forum*, Berlin, Germany, Sept. 1999.

[3]Orchard, M. N., and Newman, S. J., "The Compound Helicopter—Why Have We Not Succeeded Before?," *The Aeronautical Journal of the Royal Aeronautical Society*, Vol. 103, No. 1028, Oct. 1999, pp. 489–495.

[4]Lynn, R. R., "Wing Rotor Interactions," *Journal of Aircraft*, Vol. 3, No. 4, 1966, pp. 326–332.

[5]Carlson, R. M., "Possibilities of Compound Rotorcraft—Status 1968," *The Aeronautical Journal of the Royal Aeronautical Society*, Vol. 72, Dec. 1968, pp. 1029–1044.

[6]Fradenburgh, E. A., and Chuga, G. M., "Flight Program of the NH-3A Research Helicopter," *Journal of the American Helicopter Society*, Vol. 13, No. 1, 1968, pp. 44–62.

[7]Arcidiacono, P. J., deSimone, G., and Occhiato, J., "Preliminary Evaluation of RASA Data Comparing Pure Helicopter, Auxiliary Propulsion and Compound Helicopter Flight Characteristics," *Journal of the American Helicopter Society*, Vol. 27, No. 1, 1982, pp. 42–51.

[8]Anderson, W. D., and Wood, E. R., "AH-56A (AMCS) Compound Helicopter Vibration Reduction," *Proceedings of the 30th Annual Forum of the American Helicopter Society*, Washington, DC, May 1974.

[9]Balmford, D. E. H., "Some Reflections on Trends in Rotorcraft Technology and Configurations—into the 21st Century," *Aeronautical Journal*, Vol. 98, No. 974, April 1994, pp. 113–126.

[10]Humpherson, D. V., "Compound Interest—A Dividend for the Future, Revised," *Presented at the 54th Annual Forum of the American Helicopter Society*, Washington, DC, May 1998.

[11]Bir, G., et al., "University of Maryland Advanced Rotorcraft Code (UMARC) Theory Manual," Univ. of Maryland, UM-AERO Rept. 94-18, College Park, July 1994.

[12]Spreuer, W. E., "Experimental Flight Tests of The XH-51A Compound Helicopter," *Journal of the American Helicopter Society*, Vol. 13, No. 1, 1968, pp. 64–69.

[13]Drees, J. M., "High Speed Helicopter Rotor Design," *Proceedings of the 19th Annual Forum of the American Helicopter Society*, Washington, DC, May 1963.

[14]Johnson, W., "Helicopter Theory," Dover, New York, 1980, Chap. 4–5.

[15]Tauszig, L., "Numerical Detection and Characterization of Blade-Vortex Interactions Using a Free Wake Analysis," M.S. Thesis, Dept. of Aerospace Engineering, Pennsylvania State Univ., University Park, Aug. 1998.

[16]Foulke, W. K., and Rhodes, J. E., "The XH-51A Rigid Rotor Compound Helicopter," *Proceedings of the 21st Annual Forum of the American Helicopter Society*, Washington, DD, May 1965.

[17]Tanner, W. H., and Bergquist, R. R., "Some Problems of Design and Operation of a 250-Knot Compound Helicopter Rotor," *Journal of Aircraft*, Vol. 1, No. 5, 1964, pp. 252–259.